Online Submissions: wjg.wjgnet.com
wjg@wjgnet.com
doi:10.3748/wjg.15.6044

World J Gastroenterol 2009 December 28; 15(48): 6044-6051
World Journal of Gastroenterology ISSN 1007-9327

ORIGINAL ARTICLE

MRI *versus* 64-row MDCT for diagnosis of hepatocellular carcinoma

Michael Bernhard Pitton, Roman Kloeckner, Sascha Herber, Gerd Otto, Karl Friedrich Kreitner, Christoph Dueber

Michael Bernhard Pitton, Roman Kloeckner, Sascha Herber, Karl Friedrich Kreitner, Christoph Dueber, Department of Diagnostic and Interventional Radiology, Johannes Gutenberg-University, Langenbeckstr. 1, 55131 Mainz, Germany
Gerd Otto, Department of Transplantation and Hepatobiliopancreatic Surgery, University of Mainz, Langenbeckstr. 1, 55131 Mainz, Germany
Author contributions: Pitton MB and Herber S read the CT and MRI scans; Pitton MB and Kloeckner R wrote the paper; Kreitner KF implemented the MRI protocol and conducted the scans; Otto G performed the liver transplantations; Dueber C was the supervisor, provided the resources and made the project possible.
Correspondence to: Michael Bernhard Pitton, Professor of Radiology, Department of Diagnostic and Interventional Radiology, Johannes Gutenberg-University, Langenbeckstr. 1, 55131 Mainz, Germany. pitton@radiologie.klinik.uni-mainz.de
Telephone: +49-6131-172057 Fax: +49-6131-176633
Received: June 30, 2009 Revised: August 31, 2009
Accepted: September 7, 2009
Published online: December 28, 2009

Abstract

AIM: To compare the diagnostic capability of multidetector computed tomography (MDCT) and magnetic resonance imaging (MRI) for the detection of hepatocellular carcinoma (HCC) tumour nodules and their effect on patient management.

METHODS: A total of 28 patients (25 male, 3 female, mean age 67 ± 10.8 years) with biopsy-proven HCC were investigated with 64-row MDCT (slice 3 mm native, arterial and portal-venous phase, 120 mL Iomeprol, 4 mL/s, delay by bolus trigger) and MRI (T1fs fl2d TE/TR 2.72/129 ms, T2tse TE/TR 102/4000 ms, 5-phase dynamic contrast-enhanced T1fs fl3d TE/TR 1.56/4.6, Gadolinium-DTPA, slice 4 mm). Consensus reading of both modalities was used as reference. Tumour nodules were analyzed with respect to number, size, and location.

RESULTS: In total, 162 tumour nodules were detected by consensus reading. MRI detected significantly more tumour nodules (159 *vs* 123, $P < 0.001$) compared to MDCT, with the best sensitivity for early arterial phase MRI. False-negative CT findings included nodules ≤ 5 mm ($n = 5$), ≤ 10 mm ($n = 17$), ≤ 15 mm ($n = 12$), ≤ 20 mm ($n = 4$), and 1 nodule > 20 mm. MRI missed 2 nodules ≤ 10 mm and 1 nodule ≤ 15 mm. On MRI, nodule diameters were greater than on CT (29.2 ± 25.1 mm, range 5-140 mm *vs* 24.1 ± 22.7 mm, range 4-129 mm, $P < 0.005$). In 2 patients, MDCT showed only unilobar tumour spread, whereas MRI revealed additional nodules in the contralateral lobe. Detection of these nodules could have changed the therapeutic strategy.

CONCLUSION: Contrast-enhanced MRI is superior to 64-row MDCT for the detection of HCC nodules. Patients should be allocated to interventional or operative treatment according to a dedicated MRI-protocol.

Key words: American Association for the Study of Liver Diseases; European Association for the Study of the Liver; Hepatocellular carcinoma; Multidetector computed tomography; Magnetic resonance imaging

Peer reviewer: Paul E Sijens, PhD, Associate Professor, Radiology, UMCG, Hanzeplein 1, 9713GZ Groningen, The Netherlands

Pitton MB, Kloeckner R, Herber S, Otto G, Kreitner KF, Dueber C. MRI *versus* 64-row MDCT for diagnosis of hepatocellular carcinoma. *World J Gastroenterol* 2009; 15(48): 6044-6051 Available from: URL: http://www.wjgnet.com/1007-9327/15/6044.asp DOI: http://dx.doi.org/10.3748/wjg.15.6044

INTRODUCTION

Hepatocellular carcinoma (HCC) is the fifth most common cancer in the world and the third most common cause of cancer death, with 600 000 to 1 million new cases being diagnosed each year[1,2]. In North America and Europe, the most common risk factors are alcoholic cirrhosis and chronic hepatitis C and hepatitis B infection[3-6]. Patient survival has not significantly improved in the last 30 years because most cases are still not diagnosed until the disease is already in an advanced stage, which limits the most effective therapeutic options[7]. Therefore, early tumour detection is one of the most important issues in HCC therapy[8]. Currently, magnetic

resonance imaging (MRI) and multidetector computed tomography (MDCT) are both equally used for HCC diagnosis, although in the past MRI has been reported to produce significantly higher detection rates[9-11]. State-of-the-art MRI provides fast imaging techniques with dynamic contrast-enhanced sequences to detect the mostly hypervascularized HCC tumour nodules with a high sensitivity and specificity. However, current developments in MDCT techniques provide better spatial resolution than MRI and quick scan times potentially cause fewer motion artifacts and improve the accuracy of MDCT. The exact number and the distribution of tumour nodules is crucial for allocating these patients to adequate treatment regimens; however, it is well known that particularly small nodules often remain undetected using radiological methods[8,12,13]. The purpose of this study was to compare the diagnostic capability of 64-row MDCT and MRI for the detection of hypervascularized tumour nodules in the cirrhotic liver to allow for adequate treatment.

MATERIALS AND METHODS

Between July 2006 and July 2007, 28 patients with a suspected diagnosis of HCC on ultrasound or CT (25 male, 3 female, mean age 67.0 ± 10.8 years, range 46-89 years) were included in the study protocol. Diagnosis was confirmed by liver biopsy of at least one of the tumour nodules in 25 cases (Table 1). According to the guidelines of the European Association for the Study of the Liver (EASL), the other 3 patients were diagnosed with two different imaging techniques by arterial hypervascularization of nodules > 2 cm and/or a corresponding increase in serum levels of alpha-feto-protein[14]. For final diagnosis, all patients were included in this comparative imaging protocol that comprised contrast-enhanced MDCT and MRI in order to evaluate number, size, and location of HCC tumours for subsequent treatment allocation. The study protocol was approved by the local ethical review board. All patients gave their informed consent before entering the study.

The CT diagnosis was based on a triphasic contrast-enhanced protocol using a 64-row MDCT scanner (Brilliance 64®, Philips Medical Systems, Eindhoven, Netherlands, 120 kV, 200 mAs, collimation 64 mm × 0.6 mm, pitch 0.625, reconstruction interval 1.172 mm, slice thickness 5 mm native and 3 mm in contrast-enhanced phases). 1 mm slices were reconstructed for CT-angiography of liver arteries if the patients were considered for surgery. The contrast bolus consisted of 120 mL Iomeprol (Imeron 300®, Altana Pharma, Konstanz, Germany) administered at a flow rate of 4 mL/s using a bolus trigger technique (positioning of the respective region of interest (ROI) in the abdominal aorta just above the celiac trunk, threshold 150 Hounsfield Units (HU), start delay 10 s). The portal phase started with a delay of 50 s after reaching the threshold.

MRI was performed using a 1.5-Tesla MR scanner (Magnetom Vision®, Siemens Medical Solutions, Erlangen, Germany; software: syngo MR 2004A 4VA25A) with two body coils (CP Body Array Flex®). The study protocol covered (1) T1w-2D-Flash fatsat (TE/TR 2.72/129 ms, flip 70° , slice 6 mm, matrix 256*), (2) T2w TSE (TE/TR 102/4000 ms, flip 150° slice thickness 6 mm, matrix 256*), (3) in phase and out of phase (TE/TR 2.36/4.76/108 ms, flip 70°, slice 6 mm, matrix 256*), and (4) five dynamic contrast-enhanced T1w-3D-Flash fat sat sequences (TE/TR 1.56/4.6 ms, flip 15°, slice 4 mm, matrix 256*) with 0, 20, 45, 90, and 300 s start delay after contrast material injection (0.1 mmol/kg Gadolinium-DTPA (Magnevist®, Bayer Schering Pharma AG, Berlin, Germany), 2 mL/s by power injector (Spectris®, Medrad, Dusseldorf, Germany).

All phases of the MDCT and MRI scans were independently analyzed by two independent investigators with respect to the number, size, and location of the tumours. Both investigators had at least 10 years experience in evaluating HCC in daily practice. In order to gain the highest diagnostic sensitivity, each nodule was rated positive whenever CT or MRI or both modalities were equivocally positive by both investigators in consensus. Positive diagnosis was based on the EASL and American Association for the Study of Liver Diseases (AASLD) guidelines which require hypervascularization in

Table 1 Demographics, aetiology of liver cirrhosis and clinical condition of the patients (*n* = 28)

	n
Gender	
Male	25
Female	3
Mean age (yr)	67.0 ± 10.8 (range 46-89)
Aetiology of liver cirrhosis	
Ethanol	13
Hepatitis B	2
Hepatitis C	7
Cryptogenetic	6
Clinical stage	
BCLC stage	
A	6
B	22
C	0
D	0
Child Pugh	
A	24
B	4
C	0
Okuda	
I	25
II	3
III	0
ECOG	
0	26
I	2
II	0
III	0
IV	0
Histological tumour grading	
Well	16
Moderate	4
Poor	2
Unknown	3
No biopsy	3

BCLC: Barcelona Clinic Liver Cancer; ECOG: Eastern Cooperative Oncology Group.

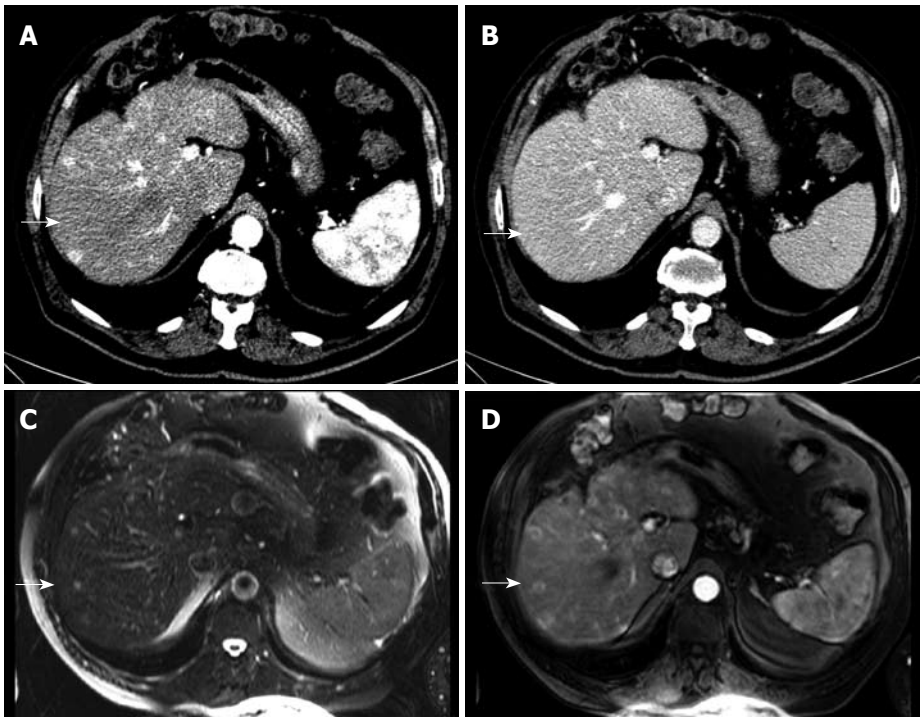

Figure 1 71-year-old man with biopsy-proven hepatocellular carcinoma (HCC). Detection of an additional tumor nodule by magnetic resonance imaging (MRI), size 12 mm (size category ⩽ 15 mm). Multi-detector computed tomography (MDCT) demonstrates two hypervascularized tumor nodules in the contrast-enhanced arterial phase (A, arrow) but not in the portal venous phase (B, arrow). MRI arterial phase depicts one more tumor nodule (arrows) in the T2w (C) and the T1w contrast-enhanced early arterial phase (D).

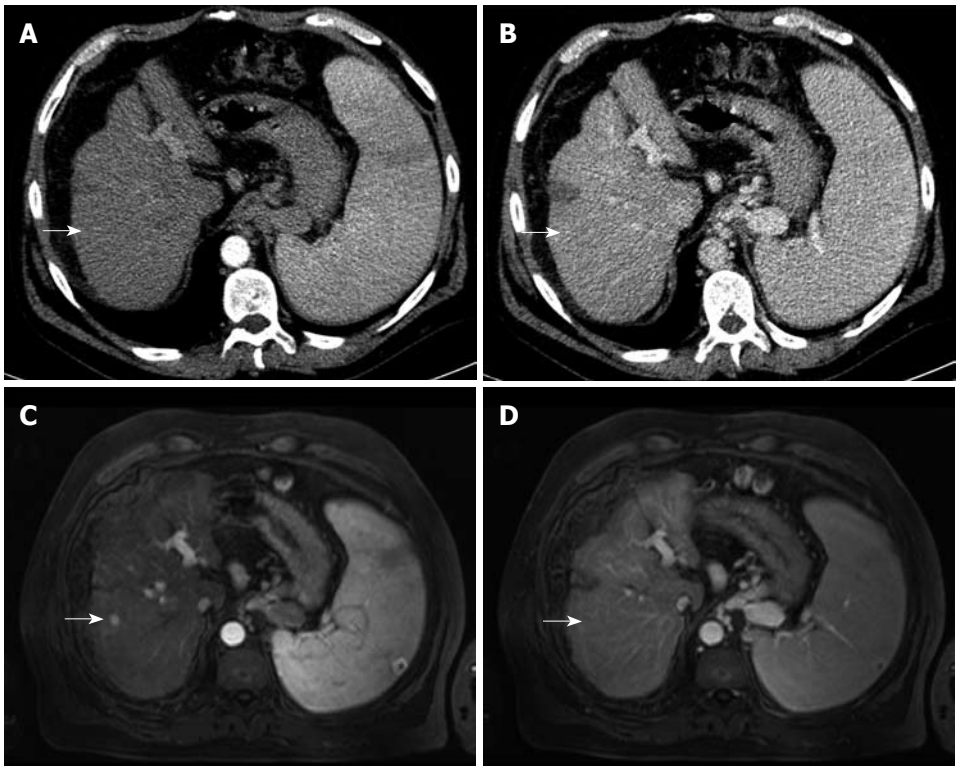

Figure 2 70-year-old man with biopsy-proven HCC. Detection of an additional tumour nodule by MRI, size 10 mm (size category ⩽ 10 mm). MDCT does not show any contrast enhancement in the arterial (A, arrow) or portal venous phase (B, arrow). MRI arterial phase depicts one more tumour nodule (C, arrow) which is hypo- to isointense on the portal venous phase (D, arrow).

arterial phase and contrast washout in the early or delayed venous phase[15]. All but three cases were histologically proven by biopsy from one representative nodule. Biopsy proof from each nodule, however, is not feasible *in vivo* due to ethical reasons. The other three cases were not histologically proven because of poor coagulation status and inappropriate subcapsular location for biopsy in order to avoid tumor cell spreading. However, these cases fulfilled the diagnosis criteria according to EASL (hypervascularized nodules > 2 cm in two imaging modalities).

All images were analyzed on a separate workstation with magnification. Tumour diameters were sized with a measuring tool integrated in the workstation software. All nodules visible in both modalities were compared in size. Additionally, the influence of HCC aetiology on tumour detection was analysed. Explanted liver specimens from patients who underwent liver transplantation (3 ×) or hemihepatectomy (1 ×) were analyzed pathologically. The specimens were cut in 4 mm slices in the same orientation as in CT and MRI in order to compare the findings. All nodules found by the

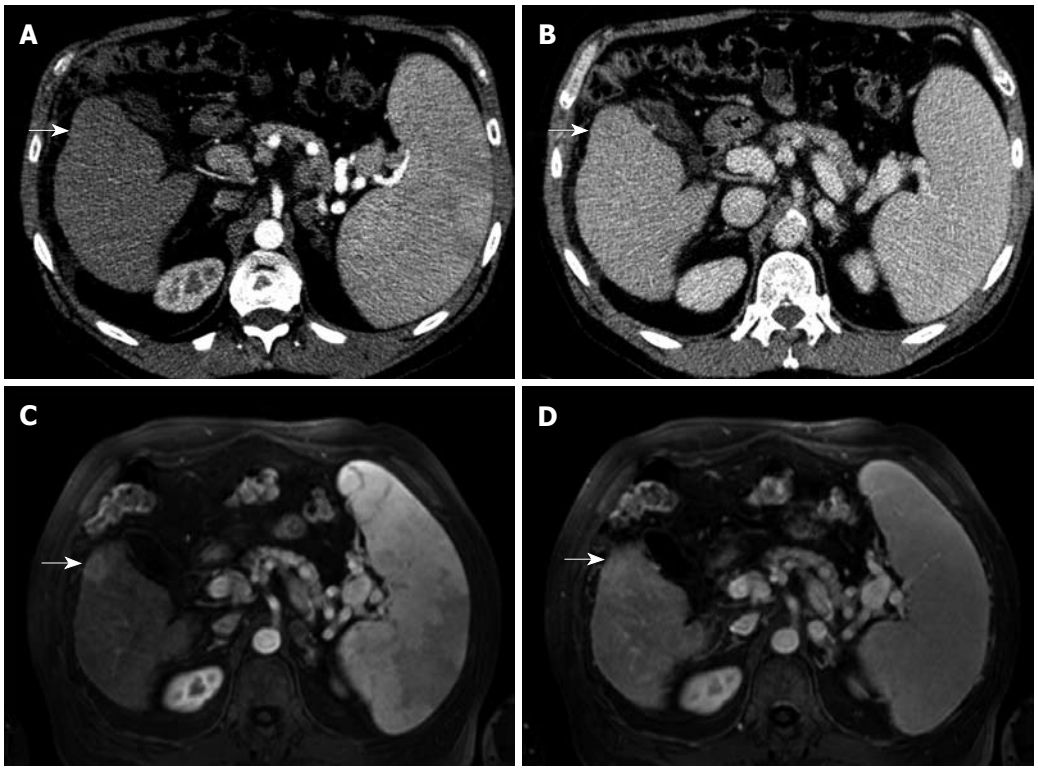

Figure 3 70-year-old man with biopsy-proven HCC. Detection of an additional tumour nodule by MRI, size 19 mm (size category ≤ 20 mm). MDCT demonstrates no hypervascular enhancement in the contrast-enhanced arterial phase (A, arrow) or the portal venous phase (B, arrow). MRI arterial phase depicts a hypervascularized area in the T1w phase (C, arrow) which became isointense in the portal venous phase (D, arrow).

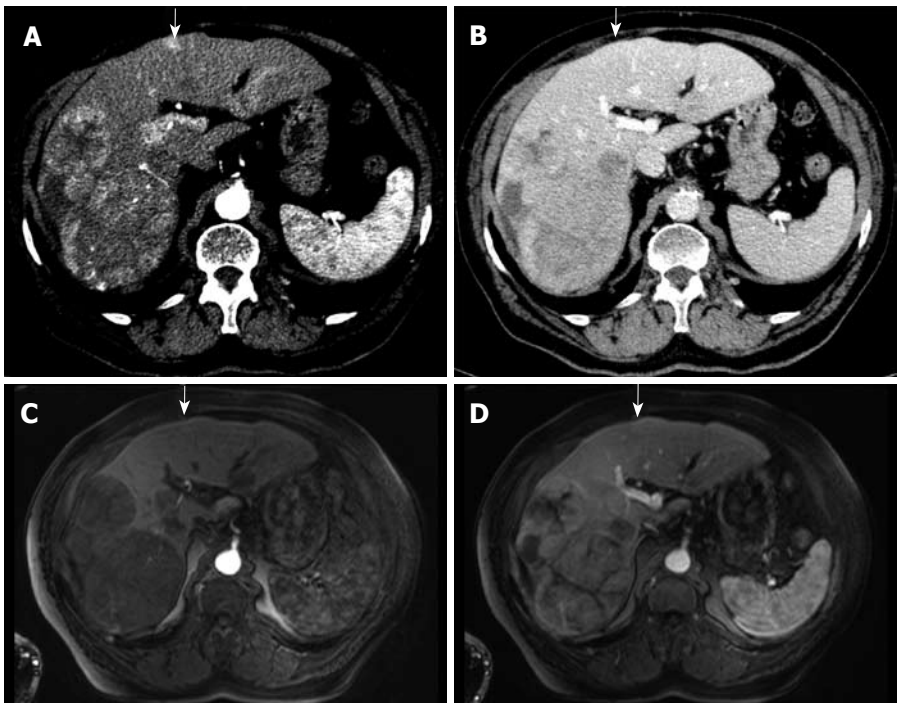

Figure 4 82-year-old man with biopsy-proven HCC. Detection of an additional tumour nodule by MDCT. The contrast-enhanced arterial phase MDCT demonstrates large tumours in the right liver lobe and one additional hypervascularized nodule in segment 4 (A, arrow) but not in the portal venous phase (B, arrow). Contrast-enhanced MRI depicts the large tumours in the right liver lobe but not in segment 4 (arrows) in early arterial phase (C) and portal venous phase (D).

pathologist were correlated to the CT and MRI data and investigated histologically.

Statistical analysis

Sensitivity for tumour detection was calculated with "R" (R: A Language and Environment for Statistical Computing, R Foundation for Statistical Computing, Version 2.5.0, Vienna, Austria, 2007), including Geepack (Generalized Estimating Equations). *P* values less than 0.05 were considered statistically significant. Statistical testing was performed by an independent statistician to avoid review bias.

RESULTS

Consensus reading of MRI and MDCT depicted a total of 162 nodules. On a per nodule basis, MRI detected

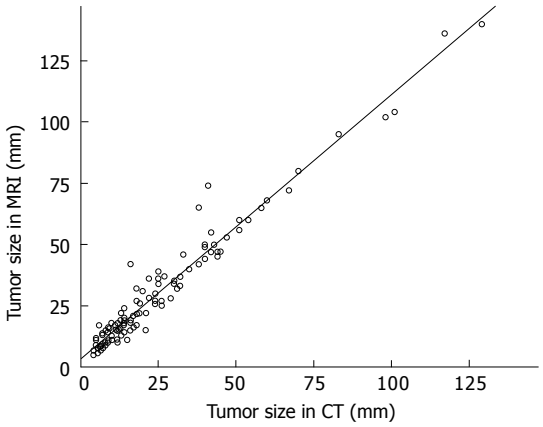

Figure 5 Correlation of tumor sizes measured with MDCT and MRI using a scatterplot. There is a tendency towards greater diameters on MRI compared to MDCT (y = 1.08x + 3.2).

Table 2 Diagnostic impact of imaging protocols on tumour detection *n* (%)

Imaging protocols of MDCT and MRI	Tumour nodules detected
MRI, T1w 3D-Flash, arterial phase (20 s start delay)	158 (97.5)
MRI, T1w 3D-Flash, portal-venous phase (45 s start delay)	145 (89.5)
MRI, T1w 3D-Flash, equilibrium phase (90 s start delay)	127 (78.4)
MDCT, arterial phase (bolus trigger for start delay)	119 (73.5)
MRI, T1w 3D-Flash, delayed phase (300 s start delay)	115 (71.0)
MRI, T1w 3D-Flash, dynamic phase Phase (T1 native)	109 (67.3)
MRI, T1w 2D Flash native	104 (64.2)
MRI, Dual-GRE in-phase	98 (60.5)
MRI, Dual-GRE out-phase	96 (59.3)
MDCT, portal-venous phase (55 s start delay)	84 (51.9)
MRI, T2w TSE	72 (44.4)
MDCT, native phase	56 (34.6)

MDCT: Multidetector computed tomography; MRI: Magnetic resonance imaging.

significantly more nodules than MDCT (159 *vs* 123, $P \leqslant 0.001$, Figures 1-3), resulting in an overall sensitivity of 0.98 for MRI and 0.76 for MDCT. The best diagnostic sensitivity was ascertained for the early arterial phase MRI, followed by portal venous phase MRI, equilibrium phase MRI, arterial phase MDCT, and late phase contrast enhanced MRI (Table 2). For native MRI phases (T1w, T2w, Dual-GRE in/out phase) and native and portal venous MDCT phases, sensitivities were low. Negative MDCT findings included 5 nodules $\leqslant$ 5 mm, 17 nodules $\leqslant$ 10 mm, 12 nodules $\leqslant$ 15 mm, 4 nodules $\leqslant$ 20 mm, and 1 nodule greater than 20 mm. In contrast, MRI missed two nodules $\leqslant$ 10 mm and one nodule $\leqslant$ 15 mm. With respect to unilobular and bilobular tumour dissemination, MRI detected 7 MDCT-negative nodules in 2 patients which were located in the contralateral liver lobe and could have changed the therapeutic strategy if not detected. In contrast, the three nodules missed in MRI (Figure 4) had no influence on the treatment regimen because the patient had multinodular disease in both lobes.

Figure 5 shows the sizes of the nodules positive in both, CT and MRI. Compared to MDCT, the diameters of the tumour nodules were slightly greater in MRI (29.2 $\pm$ 25.1 mm *vs* 24.1 $\pm$ 22.7 mm, $P < 0.005$, Figure 5). The median lesion diameter was 15.5 mm (range 5 mm to 140 mm) in MRI compared to 12 mm (range 4 mm to 129 mm). Irrespective of the false-negative MDCT findings, tumour diameters were underestimated with MDCT in 43 nodules compared to MRI. In contrast, MRI underrated tumour diameter in only one case compared to MDCT (Table 3).

During the study period, three patients underwent liver transplantation and one was allocated to hemihepatectomy. The explanted specimens (three complete organs and one right liver lobe) were transected in 4 mm slices in transverse orientation for a comparative correlation with the respective MDCT and MRI slices (Figure 6). These four specimens revealed a total number of 20 tumour nodules, 16 of which were depicted by MRI (80%) and only 13 by MDCT (65%).

DISCUSSION

The main reason for the poor survival of HCC patients is the fact that most cases are not diagnosed until disease has reached an advanced stage, which limits the most effective therapeutic options[7]. HCC cases that fulfil the Milan criteria (one nodule < 5 cm or three nodules < 3 cm) might be indicated for liver transplantation with curative intention because it not only completely removes the tumour but also the critical precancerous liver cirrhosis[8]. However, a significant number of additional intrahepatic tumours have been missed in comparative radiological studies, particularly small nodules < 20 mm[8,13,16], calling the decision-making process into question. Moreover, resection and local tumour ablation with percutaneous ethanol injection (PEI) or radiofrequency ablation (RFA) might have curative potential if the tumour nodules are not multilocular and do not exceed defined nodule diameters[17]. Thus, for optimal treatment allocation, current efforts in diagnostic work-up focus on increasing the correctness of preoperative diagnosis with respect to number, size, and location of tumour nodules.

The purpose of the present study was to evaluate the diagnostic potential of 64-row MDCT and MRI for the detection of hypervascularized tumour nodules in the cirrhotic liver for adequate treatment allocation of HCC patients. MDCT has advantages compared to MRI, such as fewer motion artifacts due to much shorter scanning time (3 to 5 s *vs* 18-25 s) and higher spatial in-plane resolution (512* *vs* 256* Matrix). However, overall sensitivity of state-of-the-art 64-row MDCT has been demonstrated to be significantly inferior compared to contrast-enhanced MRI and thereby confirms respective findings from older studies with less sophisticated CT technology[9-11,18,19]. Recent data have reported slightly higher detection rates for MDCT compared to MRI[20]. In our study, however, the outstanding contrast resolution of MRI scored much better with greater sensitivity particularly in small lesions of $\leqslant$ 10 mm compared to MDCT (0.95 *vs* 0.48, $P < 0.001$) which is in concordance

Table 3 Results of consensus reading of MDCT and MRI: No. of detected tumour nodules by MDCT and MRI depending on tumour size scaling

		MRI						
		Negative	≤ 5 mm	≤ 10 mm	≤ 15 mm	≤ 20 mm	> 20 mm	Total
MDCT	Negative		5	17	12	4	1	39
	≤ 5 mm		2	2[1]	2[1]			6
	≤ 10 mm	2		13	11[1]	4[1]		30
	≤ 15 mm	1		1[2]	12	11[1]	4[1]	29
	≤ 20 mm					3	9[1]	12
	> 20 mm						46	46
	Total	3	7	33	37	22	60	162

[1]Nodules which appeared greater in MRI compared to CT; [2]Only the single nodule was bigger in CT compared to MRI.

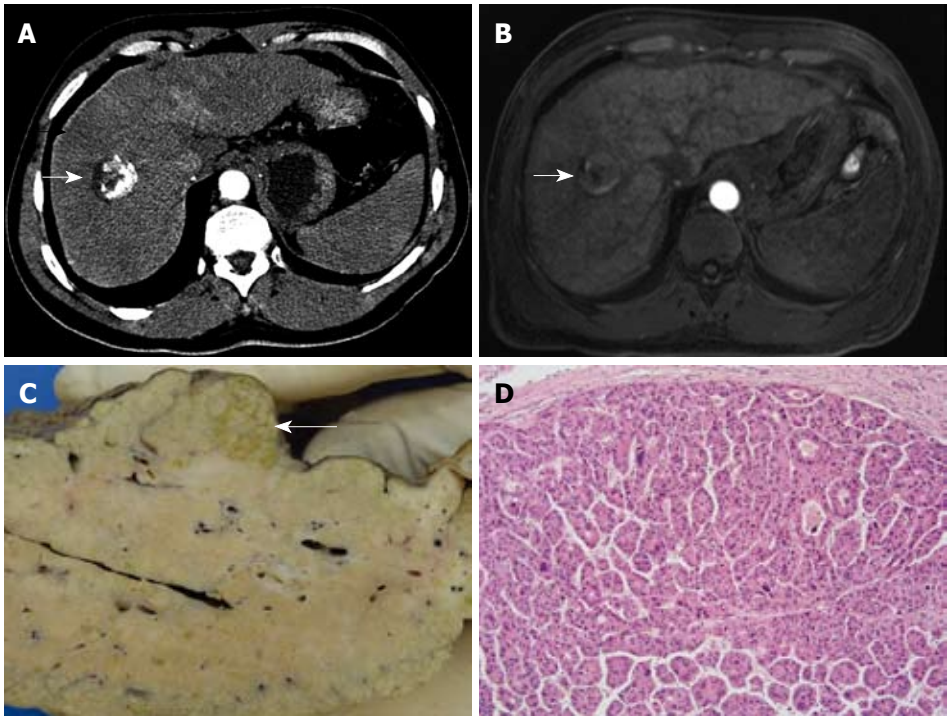

Figure 6 54-year-old man with biopsy-proven HCC. False-negative finding in the two modalities. Contrast-enhanced early arterial and portal venous phase MDCT (A) and arterial and portal venous phase MRI (B) detected a 3 cm tumour in the right liver lobe (A, B, arrows) but failed to detect another tumour nodule at the posterior surface of the left liver lobe. The explanted liver specimen clearly depicts this additional 2 cm tumour nodule on gross-sectional pathology (C, arrow) and histology (D, 10 × magnification, HE staining).

with recent reports from the literature[18,21].

Our study has some limitations. First, there was an obvious bias in patient recruitment since prior imaging results had suggested HCC in all patients before they entered the study protocol. Only 4 patients were diagnosed at an early stage with tumour nodules of small diameters so that they could be allocated to either local-ablative treatment with radiofrequency ablation or liver transplantation if they complied with the Milan criteria[8]. The majority, however, was diagnosed in an intermediate stage with multilocular disease and sometimes large tumour nodules which might have biased sensitivity. Second, the start delay for the arterial phase CT was 10 s after reaching the trigger threshold. This might have been slightly too short in light of recent reports[22] and could possibly explain the great difference between the sensitivity rates of MDCT and MRI. Third, for histological confirmation of HCC diagnosis, in most cases only one representative lesion was examined pathologically, meaning that the diagnosis of additional tumour nodules relied on imaging only. Fourth, the reference diagnosis might not actually represent the final pathological diagnosis in all cases. For example, the explanted specimen of four cases (3 × liver transplantation, 1 × hemihepatectomy) revealed a total of 20 tumour nodules, whereas MRI and MDCT had depicted only 16 and 13, respectively. So far, we have to concede that even the dedicated MRI protocol used, underrated the intrahepatic tumour spread compared to histological examination. This is consistent with the findings of previous studies which demonstrated an even worse overall tumour detection rate of around 50%-70%[8,13,16]. Fifth, the consensus reading of MDCT and MRI could have potentially overestimated nodules in MDCT and MRI by mistaking a benign hypervascularized lesion for a malignant nodule due to the lack of an absolute standard of reference. However, in light of the specimens mentioned above, the underrating of the nodule numbers

and tumour spread is still a major issue for HCC diagnosis with both modalities.

Despite these limitations, the data demonstrate that diagnostic results depend considerably on the multiphasic imaging protocols. Although the early arterial phase in MRI depicts the greatest numbers of tumour nodules[23], it potentially underestimates the real tumour spread in particular cases and might result in incorrect treatment allocation with respect to the Barcelona Clinic Liver Cancer (BCLC) classification[8,12,24-28]. Substantial efforts are required to improve the diagnostic correctness, and MRI seems to have better pre-requisites and a greater potential for future developments, either by improving MRI sequences or by employing more specific contrast materials[9,29-31], the double contrast technique[32,33] or special imaging techniques[34]. Since MDCT failed to demonstrate equivalence with MRI, triphasic contrast-enhanced MDCT protocols might only be used in the first instance. However, if CT suggests local-ablative treatment, resection, or allocation to liver transplantation, dynamic multiphasic contrast-enhanced MRI should be used in order to exclude additional tumour nodules which would probably change the initial strategy.

In conclusion, dynamic contrast-enhanced MRI is superior to triphasic 64-row MDCT for detecting numbers, sizes, and distribution of HCC tumour nodules. HCC patients should be assigned to operative or interventional treatment according to a dedicated MRI protocol.

COMMENTS

Background

Hepatocellular carcinoma (HCC) is the fifth most common cancer in the world and the third most common cause of cancer death with 600 000 to 1 million new cases being diagnosed each year. Due to the lack of specific early symptoms, most cases are not diagnosed until the disease is already in an advanced stage, which limits the most effective therapeutic options. That is why, although new treatments are available, patient survival has not significantly improved in the last 30 years. Therefore, early tumor detection is one of the most important issues in HCC therapy. The study was to compare the diagnostic capability of two imaging systems, computed tomography (CT) and magnetic resonance imaging (MRI), for tumor detection.

Research frontiers

In recent years, an enormous improvement has been taking place in the field of imaging systems. With new generations of CT and MRI scanners available, the question arised, which one is the better technique to depict this tumor.

Innovations and breakthroughs

Previous studies used older equipment, e.g. single slice CT. The advance in this study is the evaluation of a new scanner generation (64-row CT) which allows faster acquisition and therefore fewer motion artifacts with a lower slice thickness.

Applications

This article should help radiologists, gastroenterologists and other physicians dealing with HCC patients in daily practice to use the correct method of imaging in the right patient.

Peer review

The study aimed at determination of the nodule detection sensitivity of MDCT compared with MRI. The presentation of the data should be more concise.

REFERENCES

1 **Parkin DM**, Bray F, Ferlay J, Pisani P. Estimating the world cancer burden: Globocan 2000. *Int J Cancer* 2001; **94**: 153-156

2 **Liu Q**, Song Y, Zhou Y, Qiao L. A useful agent for chemoprevention of hepatocellular carcinoma? *Cancer Biol Ther* 2006; **5**: 1674-1676

3 **Bruix J**, Barrera JM, Calvet X, Ercilla G, Costa J, Sanchez-Tapias JM, Ventura M, Vall M, Bruguera M, Bru C. Prevalence of antibodies to hepatitis C virus in Spanish patients with hepatocellular carcinoma and hepatic cirrhosis. *Lancet* 1989; **2**: 1004-1006

4 **El-Serag HB**, Mason AC. Risk factors for the rising rates of primary liver cancer in the United States. *Arch Intern Med* 2000; **160**: 3227-3230

5 **Nair S**, Shiv Kumar K, Thuluvath PJ. Mortality from hepatocellular and biliary cancers: changing epidemiological trends. *Am J Gastroenterol* 2002; **97**: 167-171

6 **Bréchot C**, Thiers V, Kremsdorf D, Nalpas B, Pol S, Paterlini-Bréchot P. Persistent hepatitis B virus infection in subjects without hepatitis B surface antigen: clinically significant or purely "occult"? *Hepatology* 2001; **34**: 194-203

7 **Lodato F**, Mazzella G, Festi D, Azzaroli F, Colecchia A, Roda E. Hepatocellular carcinoma prevention: a worldwide emergence between the opulence of developed countries and the economic constraints of developing nations. *World J Gastroenterol* 2006; **12**: 7239-7249

8 **Mazzaferro V**, Regalia E, Doci R, Andreola S, Pulvirenti A, Bozzetti F, Montalto F, Ammatuna M, Morabito A, Gennari L. Liver transplantation for the treatment of small hepatocellular carcinomas in patients with cirrhosis. *N Engl J Med* 1996; **334**: 693-699

9 **Ichikawa T**. MRI in the evaluation of hepatocellular nodules: role of pulse sequences and contrast agents. *Intervirology* 2004; **47**: 252-270

10 **Tomemori T**, Yamakado K, Nakatsuka A, Sakuma H, Matsumura K, Takeda K. Fast 3D dynamic MR imaging of the liver with MR SmartPrep: comparison with helical CT in detecting hypervascular hepatocellular carcinoma. *Clin Imaging* 2001; **25**: 355-361

11 **Yamashita Y**, Mitsuzaki K, Yi T, Ogata I, Nishiharu T, Urata J, Takahashi M. Small hepatocellular carcinoma in patients with chronic liver damage: prospective comparison of detection with dynamic MR imaging and helical CT of the whole liver. *Radiology* 1996; **200**: 79-84

12 **Llovet JM**, Fuster J, Bruix J. Intention-to-treat analysis of surgical treatment for early hepatocellular carcinoma: resection versus transplantation. *Hepatology* 1999; **30**: 1434-1440

13 **Llovet JM**, Bruix J, Fuster J, Castells A, Garcia-Valdecasas JC, Grande L, Franca A, Brú C, Navasa M, Ayuso MC, Solé M, Real MI, Vilana R, Rimola A, Visa J, Rodés J. Liver transplantation for small hepatocellular carcinoma: the tumor-node-metastasis classification does not have prognostic power. *Hepatology* 1998; **27**: 1572-1577

14 **Bruix J**, Sherman M, Llovet JM, Beaugrand M, Lencioni R, Burroughs AK, Christensen E, Pagliaro L, Colombo M, Rodés J; EASL Panel of Experts on HCC. Clinical management of hepatocellular carcinoma. Conclusions of the Barcelona-2000 EASL conference. European Association for the Study of the Liver. *J Hepatol* 2001; **35**: 421-430

15 **Bruix J**, Sherman M. Management of hepatocellular carcinoma. *Hepatology* 2005; **42**: 1208-1236

16 **Burrel M**, Llovet JM, Ayuso C, Iglesias C, Sala M, Miquel R, Caralt T, Ayuso JR, Solé M, Sanchez M, Brú C, Bruix J; Barcelona Clínic Liver Cancer Group. MRI angiography is superior to helical CT for detection of HCC prior to liver transplantation: an explant correlation. *Hepatology* 2003; **38**: 1034-1042

17 **Dettmer A**, Kirchhoff TD, Gebel M, Zender L, Malek NP, Panning B, Chavan A, Rosenthal H, Kubicka S, Krusche S, Merkesdal S, Galanski M, Manns MP, Bleck JS. Combination of repeated single-session percutaneous ethanol injection and transarterial chemoembolisation compared to repeated single-session percutaneous ethanol injection in patients with non-resectable hepatocellular carcinoma. *World J Gastroenterol* 2006; **12**: 3707-3715

18 **Kim YK**, Kim CS, Chung GH, Han YM, Lee SY, Chon SB, Lee JM. Comparison of gadobenate dimeglumine-enhanced dynamic MRI and 16-MDCT for the detection of hepatocellular carcinoma. *AJR Am J Roentgenol* 2006; **186**: 149-157

19 **Noguchi Y**, Murakami T, Kim T, Hori M, Osuga K, Kawata S, Kumano S, Okada A, Sugiura T, Nakamura H. Detection of hepatocellular carcinoma: comparison of dynamic MR imaging with dynamic double arterial phase helical CT. *AJR Am J Roentgenol* 2003; **180**: 455-460

20 **Zhao H**, Yao JL, Wang Y, Zhou KR. Detection of small hepatocellular carcinoma: comparison of dynamic enhancement magnetic resonance imaging and multiphase multirow-detector helical CT scanning. *World J Gastroenterol* 2007; **13**: 1252-1256

21 **Rode A**, Bancel B, Douek P, Chevallier M, Vilgrain V, Picaud G, Henry L, Berger F, Bizollon T, Gaudin JL, Ducerf C. Small nodule detection in cirrhotic livers: evaluation with US, spiral CT, and MRI and correlation with pathologic examination of explanted liver. *J Comput Assist Tomogr* 2001; **25**: 327-336

22 **Sultana S**, Awai K, Nakayama Y, Nakaura T, Liu D, Hatemura M, Funama Y, Morishita S, Yamashita Y. Hypervascular hepatocellular carcinomas: bolus tracking with a 40-detector CT scanner to time arterial phase imaging. *Radiology* 2007; **243**: 140-147

23 **Hecht EM**, Holland AE, Israel GM, Hahn WY, Kim DC, West AB, Babb JS, Taouli B, Lee VS, Krinsky GA. Hepatocellular carcinoma in the cirrhotic liver: gadolinium-enhanced 3D T1-weighted MR imaging as a stand-alone sequence for diagnosis. *Radiology* 2006; **239**: 438-447

24 **Bruix J**, Llovet JM. Prognostic prediction and treatment strategy in hepatocellular carcinoma. *Hepatology* 2002; **35**: 519-524

25 **Llovet JM**, Brú C, Bruix J. Prognosis of hepatocellular carcinoma: the BCLC staging classification. *Semin Liver Dis* 1999; **19**: 329-338

26 **Llovet JM**, Fuster J, Bruix J. The Barcelona approach: diagnosis, staging, and treatment of hepatocellular carcinoma. *Liver Transpl* 2004; **10**: S115-S120

27 **De Giorgio M**, Fagiuoli S. Management of hepatocellular carcinoma. *Dig Dis* 2007; **25**: 279-281

28 **Forner A**, Real MI, Varela M, Bruix J. Transarterial chemoembolization for patients with hepatocellular carcinoma. *Hepatol Res* 2007; **37** Suppl 2: S230-S237

29 **Lencioni R**, Della Pina C, Bruix J, Majno P, Grazioli L, Morana G, Filippone A, Laghi A, Bartolozzi C. Clinical management of hepatic malignancies: ferucarbotran-enhanced magnetic resonance imaging versus contrast-enhanced spiral computed tomography. *Dig Dis Sci* 2005; **50**: 533-537

30 **Kang BK**, Lim JH, Kim SH, Choi D, Lim HK, Lee WJ, Lee SJ. Preoperative depiction of hepatocellular carcinoma: ferumoxides-enhanced MR imaging versus triple-phase helical CT. *Radiology* 2003; **226**: 79-85

31 **Hori M**, Murakami T, Kim T, Tsuda K, Takahashi S, Okada A, Takamura M, Nakamura H. Detection of hypervascular hepatocellular carcinoma: comparison of SPIO-enhanced MRI with dynamic helical CT. *J Comput Assist Tomogr* 2002; **26**: 701-710

32 **Bhartia B**, Ward J, Guthrie JA, Robinson PJ. Hepatocellular carcinoma in cirrhotic livers: double-contrast thin-section MR imaging with pathologic correlation of explanted tissue. *AJR Am J Roentgenol* 2003; **180**: 577-584

33 **Kim YK**, Kwak HS, Han YM, Kim CS. Usefulness of combining sequentially acquired gadobenate dimeglumine-enhanced magnetic resonance imaging and resovist-enhanced magnetic resonance imaging for the detection of hepatocellular carcinoma: comparison with computed tomography hepatic arteriography and computed tomography arterioportography using 16-slice multidetector computed tomography. *J Comput Assist Tomogr* 2007; **31**: 702-711

34 **Parikh T**, Drew SJ, Lee VS, Wong S, Hecht EM, Babb JS, Taouli B. Focal liver lesion detection and characterization with diffusion-weighted MR imaging: comparison with standard breath-hold T2-weighted imaging. *Radiology* 2008; **246**: 812-822

S- Editor Tian L **L- Editor** Webster JR **E- Editor** Tian L